ELSEVIER

Contents lists available at ScienceDirect

Colloids and Surfaces A

journal homepage: www.elsevier.com/locate/colsurfa



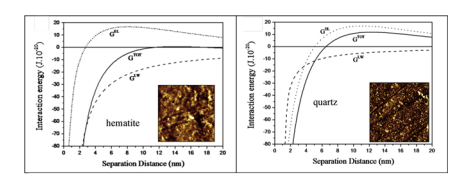
Interaction forces between colloidal starch and quartz and hematite particles in mineral flotation



Elaynne Rohem Peçanha^a, Marta Duarte da Fonseca de Albuquerque^{a,c}, Renata Antoun Simão^b, Laurindo de Salles Leal Filho^{c,d}, Marisa Bezerra de Mello Monte^{a,*}

- ^a Laboratory for Surface Chemistry, Coordination of Process and Mineral Technologies, Center for Mineral Technology CETEM, Av. Pedro Calmon, 900, Ilha da Cidade Universitária, 21941-908, Rio de Janeiro, RJ, Brazil
- b Metallurgical and Materials Engineering Program PEMM/COPPE, Federal University of Rio de Janeiro, Ilha da Cidade Universitária, 21941-972, Rio de Janeiro, RJ, Brazil
- ^c Vale Institute of Technology ITV, Avenida Juscelino Kubitschek, 31, Ouro Preto, MG, 35.400-000, Brazil
- d Laboratory of Transport Phenomena and Chemistry of Interfaces, Department of Mining and Petroleum Engineering, Av. Prof. Mello Moraes 2237, University of São Paulo, São Paulo, Brazil

GRAPHICAL ABSTRACT





ARTICLE INFO

Keywords: Starch Quartz Hematite DLVO theory AFM

ABSTRACT

In this study, we present theoretical and experimental data on the interaction forces between starch and particles of hematite and quartz as well as their implications for flotation and aggregation. The individual Hamaker constant for starch acting through vacuum, A_{11} , was calculated, and its value, 6.27×10^{-20} J, demonstrates the highly hydrophilic character of gelatinized starch. The Hamaker constants for quartz/water/starch and for hematite/water/starch, A_{132} , were also calculated, and these values were 6.07×10^{-21} J and 17.90×10^{-20} J, respectively. It was confirmed that starch strongly adsorbs onto hematite, whereas on quartz, starch may adsorb onto only silicon surface sites. In fact, AFM images of quartz surfaces showed non-adsorbed areas or areas with a thin layer of starch that certainly do not interfere in subsequent adsorption by the collector (etheramine). The interaction energies between gelatinized starch and the hematite and quartz surfaces were estimated based on DLVO theory at pH 10.5 and a constant ionic strength (10^{-3} mol.L⁻¹ NaCl). The repulsion electrostatic energy was higher for the quartz-starch system than for the interactions between hematite and starch. The calculated total energy of interaction between quartz and starch revealed that there is no possibility of aggregation for the individual colloids of starch and quartz particles. On the other hand, spontaneous adhesion between the colloids and hematite particles was confirmed by DLVO theory.

^{*} Corresponding author at: CETEM, Center for Mineral Technology, Av. Pedro Calmon, 900, Cidade Universitária, 21941-908, Rio de Janeiro, RJ, Brazil. E-mail address: mmonte@cetem.gov.br (M.B. de Mello Monte).

1. Introduction

In Brazil, reverse cationic flotation has been the most commonly used route for the concentration of itabirite [1–3]. In the process, quartz is recovered in the flotation froth in the presence of etheramine (R–O–(CH_2) $_3$ – NH_2), and the iron mineral content is usually depressed by corn starch, a mixture composed of amylopectin and amylose. For this purpose, the starch is gelatinized with sodium hydroxide. Depending on the degree of conversion of gelatinized starch and its solubility in water, it forms colloids [4].

During the preparation of the starch in sodium hydroxide solution, (i) expansion of the granules, (ii) disruption of the granules and (iii) release of the amylose into the colloidal solution occur [5]. Amylose, a polymer that forms part of the soluble fraction of the starch, has polar groups such as —COC, —OH and —COH. However, its interaction with negatively charged mineral surfaces (in particular, iron oxides) in the alkaline pH range occurs because of the hydrogen bonds between the OH groups of the starch and the hydrated mineral surface.

Our results indicate that starch undergoes an important oxidation process under industrial gelatinization conditions, which favours the binding of starch molecules. Meanwhile, the oxide surface is subjected to full hydroxylation, leading to strong polysaccharide-metal hydroxide interactions. Furthermore, Fourier transform infrared (FTIR) and X-ray photoelectron spectroscopy (XPS) spectral changes serve as evidence of surface chemical modification as starch adsorbs onto the oxide and forms a surface chemical complex. The nature of these interactions is thus assumed to not be simply related to electrostatic and chemical interactions [5–7].

One of the causes of the loss of efficiency in the reverse cationic flotation of iron ore may be related to the presence of quartz in the sunken material. The particles are not recovered by flotation, particularly for hydrodynamic reasons, and can be dragged to the bottom of the flotation cell because they are not sufficiently hydrophobic. Because amine collectors adsorb on both quartz and hematite surfaces, the selective adsorption of starch on hematite plays a key role in the selective separation of quartz–hematite [8].

The starch may also interact with the quartz particles and partially inhibit the adsorption of the collector, etheramine, reducing the hydrophobic coverage of the particles and the consequent selectivity of the process [8]. The study of the interaction between starch and quartz particles also becomes important in evaluating the competitive adsorption of this depressant between the quartz and hematite particles, a subject that has been little investigated.

In this study, we present theoretical and experimental data describing the interaction forces between starch and particles of hematite and quartz as well as their implications for flotation and flocculation. DLVO theory [9,10] was applied to predict the behaviour between particles, that is, the effects of repulsive or attractive forces. The surface potential, interfacial tension and contact angle, which are necessary for the calculation of the interaction free energy, were determined experimentally.

Another important aspect considered in this study concerns the significant concentrations of starch that are industrially employed in the reverse cationic flotation (at pH 10–10.5). In industrial tests, the optimum concentration of starch for a pulp (50%) desliming iron ore is in the range of 500–1000 ppm [11]. At these high concentrations of gelatinized starch, an increase in the size of the colloidal starch particles in the suspension is observed. One of the objectives of this study was to evaluate the size distribution of these particles as a function of the concentration of starch in the suspension and the electrokinetic properties of these particles.

The Hamaker constant for starch, which is essential for the construction of potential energy diagrams, was estimated by Hamaker microscopic theories and Lifshitz's macroscopic solid body theory.

In the present work, measurements by atomic force microscopy (AFM) were performed to visualize the interaction between starch and the hematite and quartz surfaces. These results contribute to

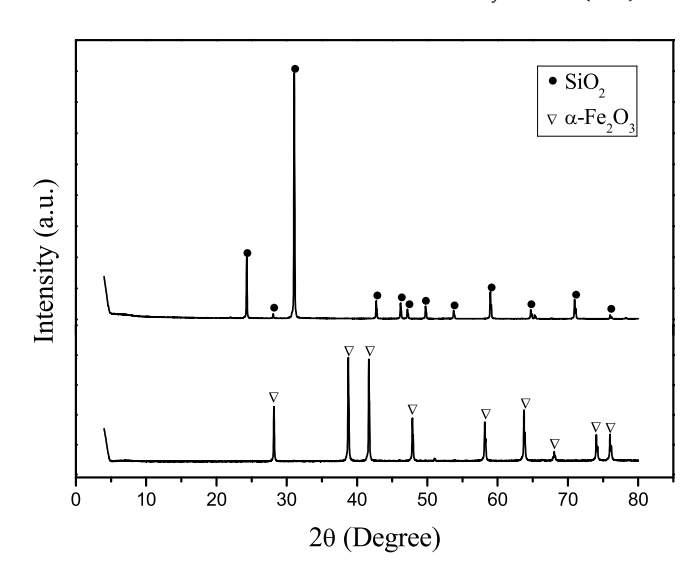


Fig. 1. X-ray diff; raction patterns of the quartz and hematite samples.

understanding the mechanisms of cationic reverse flotation and the development of new flotation processes.

2. Experimental procedures

2.1. Minerals and reagents

The hematite and quartz samples of high purity used in this study were purchased from Minas Gerais State in Brazil. Fig. 1 shows the results of X-ray diffraction analysis of quartz and hematite samples. The diffractogram shows the expected peaks for quartz and hematite, revealing that the samples were of high purity. The chemical composition of the samples determined by X-ray fluorescence (XRF) and inductively coupled plasma optical emission spectrometry (ICP-OES) is summarized in Table 1. The results indicate that the major components are Fe with minor to trace amounts of Ti, Cr, Al, Si, Ca, and Mn for the hematite sample. For the quartz samples, the main component is Si (46.32%), and they have minor amounts of Fe (0.11%) and Ca (0.22%).

All the reagents used were of analytical grade. Corn starch and etheramine were obtained from Sigma-Aldrich and Clariant, respectively. Diiodomethane was the solvent selected for the determination of the contact angle of starch. Deionized water with a specific conductance of 18 M Ω .cm was obtained from a Millipore system in the laboratory.

Table 1X-ray fluorescence (XRF) and inductively coupled plasma optical emission spectroscopy (ICP-OES) of hematite and quartz samples.

Sample	Element	Chemical analysis (%)	
		XRF	ICP
Hematite	Fe	67.6	64.80
	Ti	0.66	0.64
	Cr	0.21	0.15
	Si	0.15	0.10
	Al	0.14	0.15
	Mn	< 0.10	0.14
	Mg	< 0.10	0.04
	Ca	< 0.10	0.08
	Na	-	0.06
Quartz	Si	46.32	45.88
	Ca	0.22	0.24
	Fe	0.11	0.11
	Cr	< 0.10	0.04
	Al	< 0.10	0.02
	K	_	0.05
	Mn	_	< 0.01
	Mg	-	< 0.01

For microflotation and zeta potential tests, the mineral samples were comminuted and classified until particle sizes were in the range of -106 + 75 μ m and < 20 μ m, respectively.

Polished sections of the quartz (101) and hematite (001) $(1 \times 1 \times 2 \, \text{cm})$ samples were obtained and fixed in epoxy resin for measurements of contact angle and image analysis by means of AFM. To obtain a flat mineral surface, the surfaces of quartz (101) and hematite (001) samples were sanded and then polished with a polishing cloth purchased and a DiaDuo-2 water-based 1 μ m diamond suspension, both obtained from Struers (Ballerup, Denmark). Then, these samples were cleaned ultrasonically in ethanol and deionized water separately for 10 min, followed by gentle drying with ultrahigh purity N_2 gas.

In the conditioning steps, solutions of gelatinized starch were prepared at different concentrations. The corn starch was then gelatinized by adding a sodium hydroxide solution (10% w/w) at a ratio of 5:1. In this preparation, 1 g of corn starch was dispersed in $12\,\text{mL}$ of deionized water, and $2\,\text{mL}$ of sodium hydroxide solution was then added. After the gelatinization process, deionized water was added until a concentration of 1% w/w was reached.

For the determination of the contact angle, a gelatinized starch film was obtained. For this purpose, 50 mL of the gelatinized starch (obtained according to the methodology described above) was transferred to a 200 mL plastic beaker. A beaker containing the gelatinized starch was maintained in a vacuum desiccator at $T=25\,^{\circ}\mathrm{C}$ until a thin film formed. The value of the contact angle obtained in this experiment was used to calculate the individual Hamaker constant (A_{11}) of the gelatinized starch.

2.2. Microflotation tests

The microflotation tests were performed in a 250 ml modified Partridge-Smith tube. In this test, 2 g of mineral sample, 50 ml of a 1×10^{-3} M sodium chloride (NaCl) solution and a starch emulsion (1000 mg.L⁻¹) were used, and the resulting mixture was conditioned for 5 min. After etheramine (50 mg.L⁻¹) was added as a collector, the sample was left for 1 min. The conditioning and flotation steps were carried out at pH 10.5, and the adjustment was performed with diluted solutions of hydrochloric acid (HCl) and NaOH. The desired air flow rate was 15 mL.min⁻¹. The flotation time was 6 min. The products were filtered, dried and weighed.

2.3. Zeta potential measurements

Zeta potentials of the hematite and quartz were determined as a function of pH in the presence and absence of starch using a zeta potential analyser (Malvern Instruments–Zetasizer, Nano Series ZS). For each experiment, 0.05 g ($\sim\!20\,\mu\text{m}$) of hematite or quartz samples was conditioned in 50 mL of NaCl solution at a concentration of 1×10^{-3} M to make a $1\,g\,L^{-1}$ suspension. Then, the suspension pH was adjusted using dilute solutions of HCl and NaOH. All experiments were conducted with the pH progressively changed from 11 to 1, with 10 min of equilibration at each new pH value. In some experiments, gelatinized starch was added to the electrolyte solution to make a suspension containing 500 mg L^{-1} of starch. The zeta potential of starch colloidal particles was also determined as a function of pH using a 1×10^{-3} M NaCl solution as an indifferent electrolyte.

2.4. Dynamic light scattering experiments

Dynamic light scattering experiments were performed using a Zetasizer Nano Zs equipped with a $633\,\mathrm{nm}$ He-Ne laser; this technique determines the hydrodynamic radius of particles based on intensity fluctuations of scattered laser light. For this purpose, 1 mL of gelatinized starch emulsion was analyzed in single-use poly(methylmethacrylate) cuvettes with a path length of $12.5\,\mathrm{mm}$ after an equilibration time of $120\,\mathrm{s}$ at $25\,\mathrm{^{\circ}C}$. The mean size curves were obtained as a function

of starch concentration. The size distribution of starch colloidal particles from emulsions was determined as a function of pH using a 1×10^{-3} M NaCl solution as an indifferent electrolyte.

2.5. Atomic force microscopy (AFM)

An atomic force microscope (1 M Plus, JPK Instruments, Germany) was used to image the quartz (101) and hematite (001) samples before and after the conditioning step with gelatinized starch solution (1000 $\rm mg\,L^{-1}$) at pH 10.5 for 10 min. After this conditioning, these samples were dried using nitrogen gas.

Images were obtained in dynamic mode using a Bruker (RFESP model) cantilever with a nominal spring constant of 3.0 N/m and a scan area of $5\times 5~\mu\text{m}^2.$ The images were processed using JPK image processing V.3 software.

2.6. Contact angle measurements

Contact angle measurements were carried out on gelatinized starch films using an NRL A-100-00 Ramé-Hart Goniometer operated in air and at $T=25\,^{\circ}\text{C}$. Two different liquids were used: deionized water and diiodomethane. Starch film was cut into strips, fixed with double-sided adhesive tape and placed onto a sample holder for contact angle measurements. The sessile drop method was used. Then, a $2\,\mu\text{L}$ drop of the desired liquid was placed on the starch film surface, and measurements were recorded.

3. Results and discussion

3.1. Microflotation experiments

The recovered microflotation of quartz and hematite is shown as a function of flotation time at pH 10.5 in Fig. 2. For equivalent physicochemical conditions, the recovery of quartz was near 100% after 6 min of flotation. On the other hand, the recovery of hematite showed values close to 0% for the same flotation time. The flotation reagent system was optimized for maximum quartz recovery, while almost all of the hematite particles sank into the cell.

The recovery of hematite as a function of starch concentration was also investigated (Fig. 3). The hematite depression by the gelatinized starch occurs only at concentrations higher than $500\,\mathrm{mg.L}^{-1}$.

Fig. 4 presents the zeta potential of hematite, colloidal starch and hematite in contact with 500 mg.L⁻¹ gelatinized starch as a function of

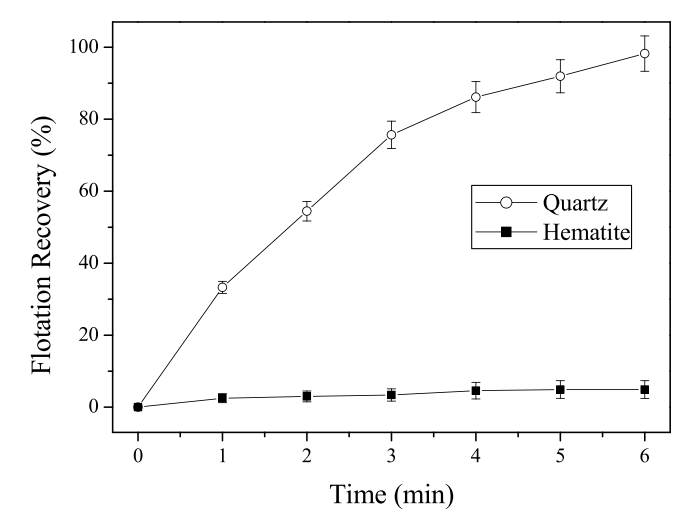


Fig. 2. Recovery of quartz and hematite as a function of flotation time ([starch] = $1000\,\mathrm{mg\,L^{-1}}$; [etheramine] = $50\,\mathrm{mg\,L^{-1}}$; pH 10.5; constant ionic strength of 1×10^{-3} M NaCl).

pH. The point of zero charge (PZC) of natural hematite was at a pH value close to 4.8. These PZC values for natural hematite agree well with values reported in the literature [12,13]. Fig. 4 also shows that the starch colloidal particles presented a PZC at \sim pH 2.8, since the counter ions Na⁺ are part of the indifferent electrolyte. At pH values above the PZC, the zeta potential values of these colloidal particles became more negative, reaching values close to $-10\,\text{mV}$ at pH 11.0. After the interaction between starch and hematite particles (Fig. 4), the profile of the zeta potential curve changes significantly, shifting to potential values close to those obtained from a colloidal starch particle zeta potential curve for samples with an indifferent electrolyte (1 \times 10 $^{-3}$ M NaCl).

The adsorption of hematite by an emulsion containing a high concentration of colloidal starch particles $(500\,\mathrm{mg\,L^{-1}})$ indicates that the chemical interaction is the major contribution to the free adsorption energy, particularly in the more alkaline range of the pH suspension. In a recent study, previously proposed starch interaction mechanisms were discussed, and the surface chemistry of starch adsorbed onto hematite was investigated by means of XPS and FTIR spectroscopy [6]. These results showed that a strong starch-hematite interaction occurs via the formation of a polysaccharide-metal hydroxide ring, suggesting the formation of a chemical complex on the hematite surface [6,7,14].

Fig. 5 shows the zeta potential of quartz in the absence and presence of $500\,\mathrm{mg.L^{-1}}$ gelatinized starch. The addition of negatively charged starch colloids causes the zeta potential to increase at pH values below the PZC of quartz (pH = 1.8). As shown in this figure, the presence of starch initially promoted changes in the zeta potential curve shape of quartz (at pH values up to nearly 5.0). In a more alkaline pH region and the presence of gelatinized starch, the quartz zeta potential values become more negative, and the curve acquires characteristics very close to the zeta potential curve of quartz in the absence of starch. At pH values above 10, the two curves come together because there is no specific adsorption of the starch on the negatively charged mineral.

Figs. 6(a) and 7 (a) show the AFM images of quartz (101) and hematite (001) surfaces after being polished using 1 μ m diamond paste [15]. The root-mean-square (RMS) roughness obtained for quartz and hematite after preparation their surfaces, was 0.96 nm and 2.42 nm, respectively. Similar values were found for the roughness for these surfaces in the literature, supporting the choice of the polishing method used in this study [16,17].

Figs. 6(b) and 7 (b) show the AFM images of quartz and hematite after conditioning with gelatinized starch solution for 10 min (at pH 10.5). According to the topographic images, non-adsorbed areas or a thin layer of starch was observed on the surface of the quartz. On the other hand, the conditioning of the surface of the hematite with gelatinized starch provided a homogeneous covering over its entire surface. After adsorption of corn starch, the root-mean-square (RMS) roughness obtained for quartz and hematite was 2.39 and 2.82, respectively. Thus, it can be concluded that the increase roughness is affected by the starch adsorption onto the mineral surfaces.

3.2. Analysis of the DLVO interaction energy

The classical DLVO [18,19] theory considers the total interaction energy (G^{TOT}) to be determined by the sum of Lifshitz-van der Waals (G^{LW}) and electrostatic (G^{EL}) interaction energies.

$$G^{TOT} = G^{LW} + G^{EL} \tag{1}$$

The van der Waals interaction is a microscopic force of attraction originating from permanent and induced electrical interactions between two or more atoms or molecules [20]. To determine the contribution from van der Waals forces, the standard expression that describes these forces between a sphere and a planar surface was used [21,22]. If the sphere and planar surface particles are considered, the non-retarded van der Waals potential energy can be evaluated by the Hamaker approximation for short distances:

$$G^{LW} = -\frac{A_{132}r}{6H} \tag{2}$$

where A_{132} is the effective Hamaker constant, r is the radius of the particle and H is the distance between the sphere and the planar surface.

The effective Hamaker constant (A_{132}) was obtained from the individual Hamaker constants for homogeneous phases:

$$A_{132} = (\sqrt{A_{11}} - \sqrt{A_{33}})(\sqrt{A_{22}} - \sqrt{A_{33}}) \tag{3}$$

where A_{11} , A_{22} and A_{33} are the Hamaker constants for media 1, 2 and 3 interacting with the same medium across vacuum.

The individual Hamaker constant, A_{11} , can be obtained from Eq. (4):

$$A_{11} = 24\pi \gamma_S^{LW}(d_0)^2 \tag{4}$$

where γ_S^{LW} is the Lifshitz-van der Waals energy component and d_0 is the minimum separation distance between the sphere and the planar surface, which is 1.65 Å [21].

A drop of an apolar liquid on a solid surface can be used to determine the Lifshitz-van der Waals interfacial tension (γ_s^{LW}) by Eq. (5) [23]:

$$\gamma_L(1+\cos\theta) = 2\sqrt{(\gamma_s^{LW}\gamma_L^{LW})} \tag{5}$$

where γ_L is the total interfacial tension of the apolar liquid, θ is the contact angle of a drop of the apolar liquid on the solid surface and γ_L^{LW} is the Lifshitz-van der Waals interfacial tension related to the apolar liquid.

The electrostatic interaction energy (G^{EL}) can be expressed by the following equation:

$$G^{EL} = \pi \varepsilon \varepsilon_0 r \left[2\zeta_1 \zeta_2 ln \left(\frac{1 + e^{-KH}}{1 - e^{-KH}} \right) + (\zeta_1^2 + \zeta_2^2) ln (1 - e^{-2KH}) \right]$$
 (6)

where ε is the dielectric constant of liquid (79); ε_0 is the permissiveness in vacuum = $8.85 \times 10^{-12} \, \text{C}^2.\text{J}^{-1}.\,\text{m}^{-1}$; r is the radius of a sphere (in m); ζ is the zeta potential valus (in V or J.C⁻¹) and H (m) is the separation distance between the particles.

The parameter 1/ K (Eq. 6) is the Debye length or the thickness of the diffuse double electrical layer (in m $^{-1}$), which depends on the Boltzmann constant $k_B=1.381\times 10^{-23}$ J. K^{-1} , absolute temperature in K (considered 295 K), electrical charge of an electron (e = 1.602×10^{-19} C), valence of ions present in solution, and number of ions present in solution (in mol. m $^{-3}$) (Equation 7).

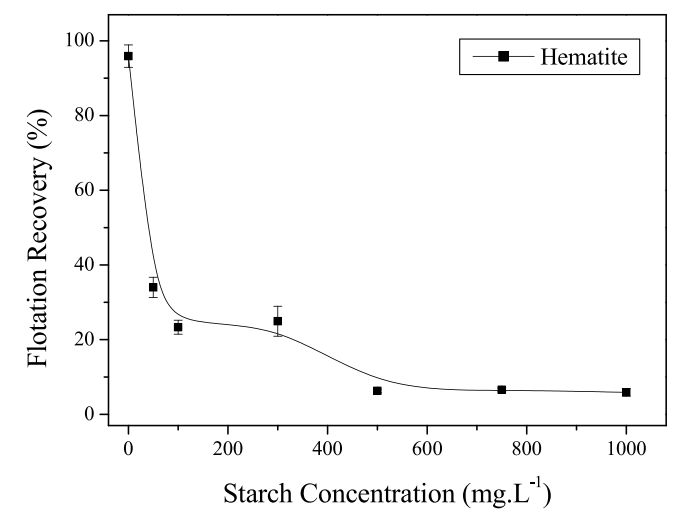


Fig. 3. Recovery of hematite after 6 min of flotation as a function of starch concentration ([etheramine] = 50 mg L^{-1} ; pH 10.5, constant ionic strength of 1×10^{-3} M NaCl).

E. Rohem Peçanha et al. Colloids and Surfaces A 562 (2019) 79–85

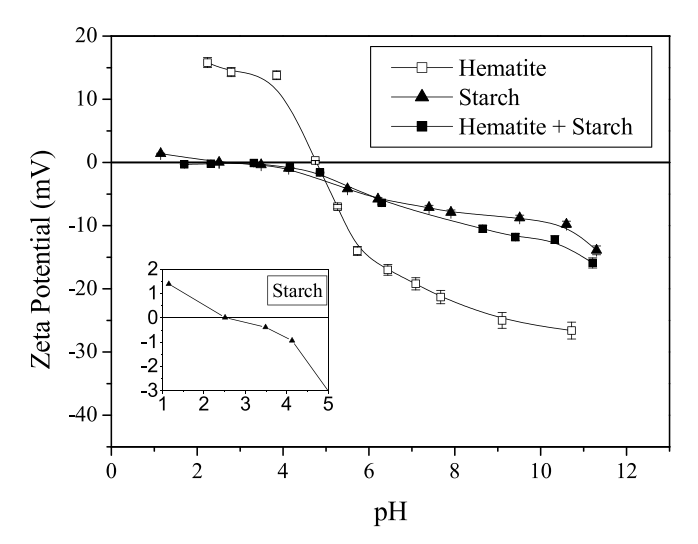


Fig. 4. Zeta potential of hematite, starch and hematite in contact with starch as a function of pH (500 mg L $^{-1}$ starch) at a constant ionic strength of 1 \times 10 $^{-3}$ M NaCl.

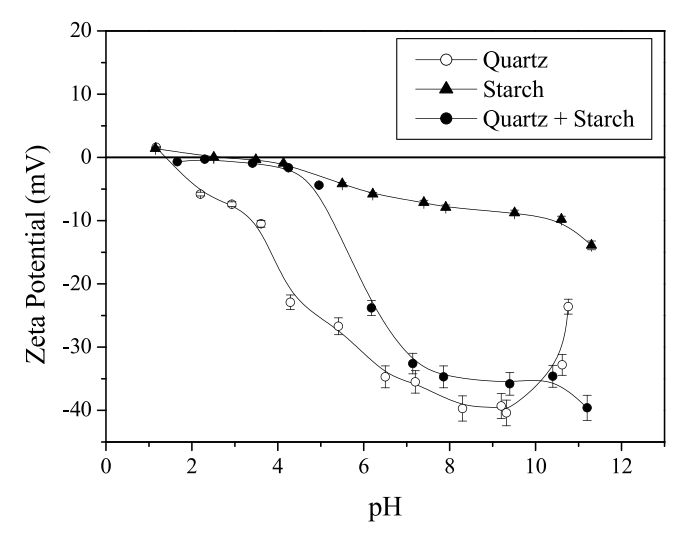


Fig. 5. Zeta potential of quartz, starch and quartz in contact with starch as a function of pH (500 mg L^{-1} starch) at a constant ionic strength of 1×10^{-3} M NaCl.

$$1/K = \left(\frac{\varepsilon \varepsilon_0 k_B T}{4\pi e^2 \sum (v_i^2 n_i)}\right)^{1/2} \tag{7}$$

The energies of interactions between gelatinized starch and the hematite and quartz surfaces were estimated based on DLVO theory [24]. The experimental procedure and the calculation of the potential energy for the development of force versus distance curves presented in the present work are described in the studies of [25] and [26].

The contact angles and the surface energy γ_S^{LW} for the gelatinized starch film are presented in Table 2. The starch film shows greater hydrophilicity in the presence of deionized water drops. The values of the Lifshitz-van der Waals energy component (γ_L^{LW}) and total energy (γ_I^T) of the diiodomethane are both 50.8 mJ.m⁻² [23].

Table 3 shows the individual and effective Hamaker constants of quartz, hematite and starch. The values of the individual Hamaker constant used in this work for hematite and quartz (A_{22}) were 25.0×10^{-20} J and 8.8×10^{-20} J, respectively [27]. The value used for the individual Hamaker water constant (A_{33}) was 3.7×10^{-20} J [23]. The Hamaker constant for starch was calculated on the basis of Equation 4.

Fig. 8 shows the size distribution as a function of gelatinized starch concentration in alkaline solution. As shown, increasing the starch concentration in the solution (from 12 ppm to 500 ppm) shifts the particle distribution curve to larger sizes. In dilute starch solutions, the particle size ranged from 100 to 300 nm. With the use of 500 ppm gelatinized starch, a significant band was observed in the diameter range between 200 and 500 nm. The value of 292 nm was used as the starch precipitate radius to calculate the electrostatic and Lifshitz-van der Waals energy components for the total interaction between colloidal starch particles and quartz/hematite surfaces.

The surface potential for each of the studied particles (quartz, hematite and starch) was estimated through zeta potential curves (see Figs. 4 and 5). These results were $-31.4\,\mathrm{mV}$ for hematite, $-35.3\,\mathrm{mV}$ for quartz and $-5.8\,\mathrm{mV}$ for gelatinized starch at pH 10.5.

The DLVO total energy curves and the electrostatic and Lifshitz-van der Waals contributions as a function of the distance between the hematite and the starch are shown in Fig. 9a. The potential curve for the electrostatic contribution showed repulsion between hematite and starch at distances ranging from approximately 2.5 to 20 nm. However, at distances less than 2.5 nm, the two surfaces converge. This result is in agreement with the values found for the zeta potential of starch and hematite at pH 10.5 (Fig. 4). On the other hand, the Lifshitz-van der Waals interaction potential presented an attractive contribution throughout the studied distance range. The total contribution of the interaction is attractive. The nature of these interactions cannot be

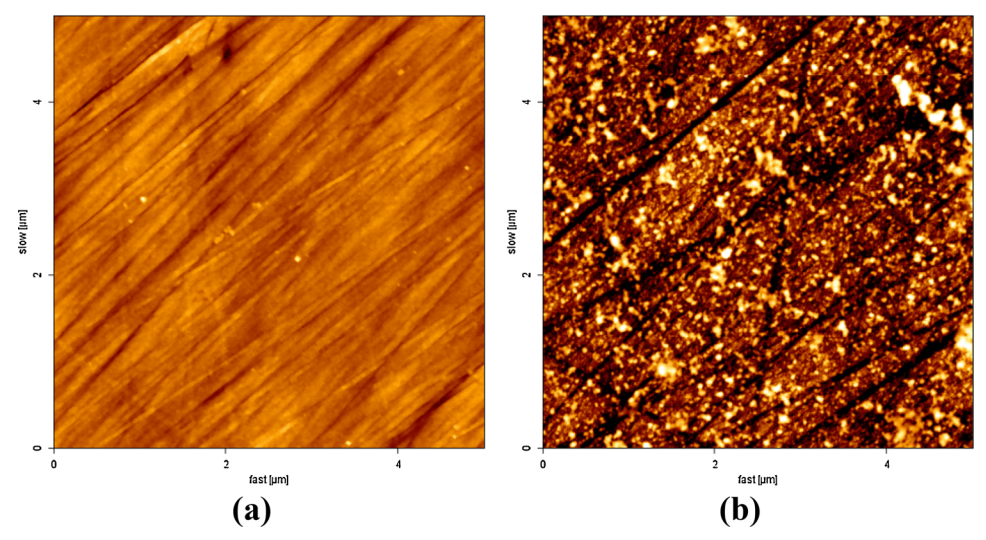


Fig. 6. AFM images of quartz topography: (a) after surface preparation and (b) after conditioning with gelatinized starch solution.

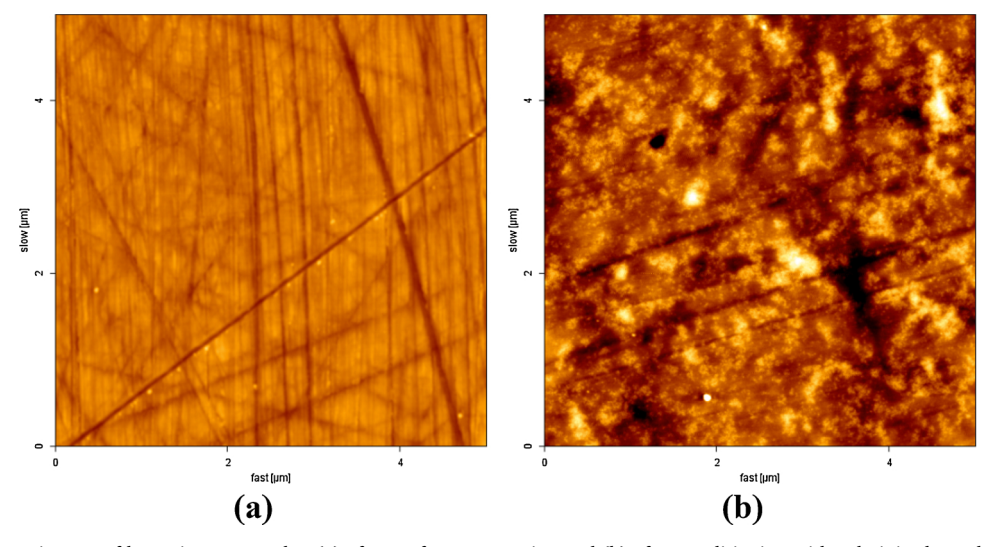


Fig. 7. AFM images of hematite topography: (a) after surface preparation and (b) after conditioning with gelatinized starch solution.

Table 2 Contact angle and surface energy (γ_S^{LW}) values for gelatinized starch film.

Starch film	
Deionized Water (°) Diiodomethane (°) γ_S^{LW} (mJ. m $^{-2}$)	60 ± 1.3 56.4 ± 1.3 30.6

Table 3 Values of individual (A_{11}, A_{22}) and effective (A_{132}) Hamaker constants.

Surface	Hamaker Constant	
Starch (A_{11}) Hematite (A_{22}) Quartz (A_{22})	$(A_{11}, A_{22}) (10^{-20} \text{J})$ 6.27 25.00 8.80	(A ₁₃₂) (10 ⁻²¹ J) - 17.90 6.07

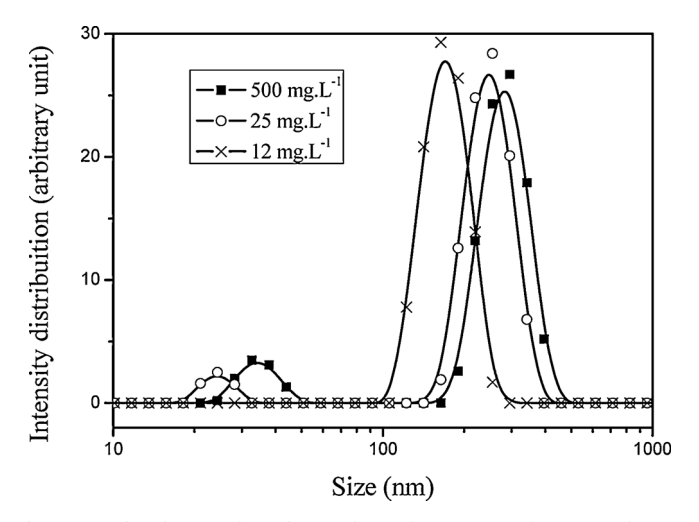
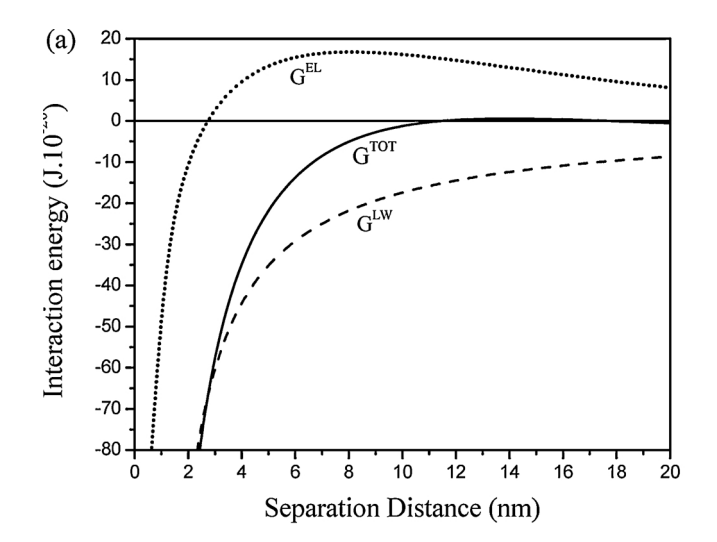


Fig. 8. Size distribution of starch particles in the presence of 1 mM NaCl at pH 10.5.

simply related to electrostatic interactions, and a chemical interaction is thus assumed to be present, in accordance with other researchers [5–7].

Fig. 9b presents the DLVO interaction potential curves as a function of the distance between quartz and starch. An attraction between quartz and starch was observed in the potential energy curve, related to the



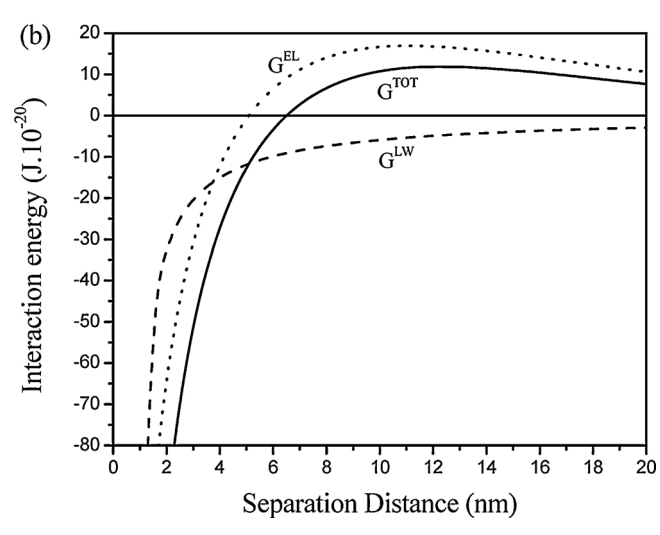


Fig. 9. Curves of calculated DLVO interaction energy between hematite and starch (a) and between quartz and starch (b) as a function of the separation distance at a constant ionic strength of 1×10^{-3} M NaCl and pH 10.5.

Lifshitz-van der Waals contribution over the entire calculated distance range. On the other hand, the curve representing the electrostatic contribution shows repulsion between the quartz surface and the starch at distances greater than 4 nm. The total contribution to the interaction energy was repulsive. The curve obtained for the DLVO interaction between quartz and starch presented an energy barrier of 11.9×10^{-20} J. Thus, the energy barrier between quartz and starch predicted by the DLVO theory is sufficiently high at pH 10.5 and prevents adhesion between these particles.

4. Conclusions

Experiments undertaken to compare the adsorption of starch onto hematite and quartz showed that starch strongly adsorbed onto hematite. It is proposed that the preferential adsorption of starch onto hematite is due primarily to the high concentration of hydroxylated iron surface sites on particles, whereas on quartz, starch may adsorb onto only silicon surface sites, particularly at pH values between 1.8 and 5.0. In a more alkaline pH region and in the presence of gelatinized starch, the quartz zeta potential values become more negative, and its zeta potential curve acquires characteristics very similar to those of the zeta potential curve of quartz in the absence of starch. At pH 10.5, the two curves overlap because there is no specific adsorption of starch on the negatively charged quartz. In fact, AFM images showed non-adsorbed areas or areas of the quartz with a thin layer of starch on the surface, which certainly does not interfere in subsequent adsorption by the collector (etheramine).

The results from microflotation experiments were compared to show that the maximum decrease in hematite (hematite floatability < 10%) occurred at starch concentrations between approximately 500 and 1000 ppm and at pH 10.5.

The size distribution of the starch colloids showed that in dilute starch solutions, the particle size ranged from 100 to 300 nm. With the use of $500\,\mathrm{mg.L}^{-1}$ gelatinized starch, significant bands in the diameter range between 200 and 500 nm were observed.

The contact angle and surface energy γ_S^{LW} (30.6 mJ.m⁻²) for the gelatinized starch film showed the same trend, i.e., higher hydrophilicity in the presence of deionized water drops.

The interaction energies between gelatinized starch and the hematite and quartz surfaces were estimated based on DLVO theory at pH 10.5 for a constant ionic strength (10^{-3} mol.L⁻¹ NaCl). The repulsion electrostatic energy was higher for the quartz-starch system than for the interactions between hematite and starch. The calculated total energy of interaction between quartz and starch revealed that there is no possibility of aggregation for the individual colloids of starch and quartz particles. On the other hand, spontaneous adhesion between the colloids and hematite particles was confirmed by DLVO theory.

Acknowledgements

The authors acknowledge Vale S/A for the samples and the CAPES and CNPq Brazilian agencies for financial support for this study.

References

[1] A.E.C. Peres, M.I. Correa, Depression of iron oxides with corn starches, Miner. Eng.

- 9 (1996) 1227-1234.
- [2] A.C. Araujo, P.R.M. Viana, A.E.C. Peres, Reagents in iron ores flotation, Miner. Eng. 18 (2005) 219–224.
- [3] N.P. Lima, E.S.V. George, A.E.C. Peres, Effect of amine and starch dosages on the reverse cationic flotation of an iron ore, Miner. Eng. 45 (2013) 180–184.
- [4] S. Yang, C. Li, L. Wang, Dissolution of starch and its role in the flotation separation of quartz from hematite, Powder Technol. 320 (2017) 346–357.
- [5] C.A. Eligwe, B.A. Okorie, C.O. Chukwudorue, F.F.O. Orumwense, The adsorption of causticized cassava starch on coal-washery effluent solids in relation to flocculation, J. Chem. Technol. Biotechnol. 42 (1988) 135–146.
- [6] G.F. Moreira, E.R. Peçanha, M.B.M. Monte, S.L. Leal Filho, F. Stavale, XPS study on the mechanism of starch-hematite surface chemical complexation, Miner. Eng. 110 (2017) 96–103.
- [7] J.S. Laskowski, Q. Liu, C.T. O'Connor, Current understanding of the mechanism of polysaccharide adsorption at the mineral/aqueous solution interface, Int. J. Miner. Process. 84 (2007) 59–68.
- [8] K. Shrimali, X. Yin, X. Wang, J.D. Miller, Fundamental issues on the influence of starch in amine adsorption by quartz, Colloids Surf. A: Physicochem. Eng. Aspects 522 (2017) 642–651.
- [9] J. Yao, H. Han, Y. Hou, E. Gong, W. Yin, A method of calculating the interaction energy between particles in minerals flotation, Math. Probl. Eng. 2016 (2016) 1–13.
- [10] K.E. Bremmell, D. Fornasiero, J. Ralston, Pentlandite-lizardite interactions and implications for their separation by flotation, Colloids Surf. A: Physicochem. Eng. Aspects 252 (2005) 207–212.
- [11] X. Ma, M. Marques, C. Gontijo, Comparative studies of reverse cationic/anionic flotation of Vale iron ore, Int. J. Miner. Process. 100 (2011) 179–183.
- [12] W. Liu, W. Liu, X. Wang, D. Wei, B. Wang, Utilization of novel surfactant N-dodecylisopropanolamine as collector for efficient separation of quartz from hematite, Sep. Purif. Technol. 162 (2016) 188–194.
- [13] D.W. Fuerstenau, D.W. Pradip, Zeta potentials in the flotation of oxide and silicate minerals, Adv. Colloid Interface Sci. 114-115 (2005) 9-26.
- [14] P.K. Weissenborn, L.J. Warren, J.G. Dunn, Selective flocculation of ultrafine iron ore. 1. Mechanism of adsorption of starch onto hematite. Colloids Surf. A: Physicochem, Eng. Aspects 99 (1995) 11–27.
- [15] H.T.B.M. Petrus, T. Hirajima, K. Sasaki, H. Okamoto, Effect of pH and diethyl dithiophosphate (DTP) treatment on chalcopyrite and tennantite surfaces observed using atomic force microscopy (AFM), Colloids Surf. A: Physicochem. Eng. Aspects. 389 (2011) 266–273.
- [16] B. Liu, X. Wang, H. Du, J. Liu, S. Zheng, Y. Zhang, J.D. Miller, The surface features of lead activation in amyl xanthate flotation of quartz, Int. J. Miner. Process. 151 (2016) 33–39.
- [17] K. Shrimali, J. Jin, B.V. Hassas, J. Wang, J.D. Miller, The surface state of hematite and its wetting characteristics, J. Colloid Interface Sci. 477 (2016) 16–24.
- [18] B.V. Derjaguin, L. Landau, Theory of the stability of strongly charged lyophobic sols and of the adhesion of strongly charged particles in solution of electrolytes, Acta Phys. Sin. 14 (1941) 633–662.
- [19] E.J. Verwey, J.T.G. Overbeek, Long distance forces acting between colloidal particles, Trans. Faraday Soc. 42 (1946) 117–123.
- [20] R.J. Hunter, Introduction to Modern Colloid Science, Oxford Science Publications, New York, 1993, p. 344.
- [21] J.N. Israelachvili, Intermolecular and Surface Forces, third ed., San Diego: Academic Press, Burlington, MA, 2011, p. 674.
- [22] H. Butt, B. Cappela, M. Kappl, Force measurements with the atomic force microscope: technique, interpretation and application, Surf. Sci. Rep. 59 (2005) 1–152.
- [23] Carel J. van Oss, Interfacial Forces in Aqueous Media, Marcel Dekker Inc., New York, 1994, p. 440.
- [24] R.M. Pashley, Interparticulate forces, in: J.S. Laskowski, J. Ralston (Eds.), Colloid Chemistry in Mineral Processing, Elsevier Science Publishing Company Inc., The Netherlands, 1992, pp. 97–113.
- [25] A. Vilinska, H.K. Rao, Surface thermodynamics and extended DLVO theory of acidithiobacillus ferrooxidans cells adhesion on pyrite and chalcopyrite, Open Colloid Sci. J. 2 (2009) 1–14.
- [26] A.E. Botero, M.L. Torem, L.M.S. Mesquita, Surface chemistry fundamentals of biosorption of Rhodococcus opacus and its effect in calcite and magnesite flotation, Miner. Eng. 21 (2008) 83–92.
- [27] F.F. Lins, A. Middea, R. Adamian, Processing of hydrophobic minerals and fine coal, Proceedings of the First UBC-McGill Bi-Annual International Symposium on Fundamentals of Mineral Processing, (1995), p. 61.